Predicting Seasonal Cycles of Atmospheric Carbon Dioxide from Global Temperature Anomalies

Wendell Tangborn
Draft Updated: December 14, 2009

Summary

Seasonal fluctuations in the concentration of atmospheric CO_2 are produced by the growth and decay of vegetation in the biosphere, which are partly controlled by global temperature variations. A major change in the atmosphere–biosphere balance that occurred during the 1977-78 climate shift is manifested by greater susceptibility of the daily change in CO_2 to global temperature variations. The underlying cause for the change is thought to be higher sea-surface temperatures during and following the climate-shift, which reduced the effectiveness of the oceans as a carbon sink (Folland, et al, 1990). Relative to the hydrosphere and biosphere, it is likely the atmosphere is now in a disequilibrium state with respect to carbon dioxide, resulting in a significant change in the interaction between temperature and atmospheric carbon dioxide (Solomon, 2007, Khatiwala, et al, 2009, Park, 2009)). Maximum and minimum daily temperature anomalies, compiled by the Hadley Climate Center at 6647 global weather stations for the 1950-2009 period, are used to predict daily changes in the concentration of atmospheric carbon dioxide. Daily changes in atmospheric CO_2 are derived from the monthly record of observations collected at Mauna Loa, Hawaii since 1958. During the past 50 years there has been a significant change in the influence of daily maximum and minimum temperature anomalies on the daily change in atmospheric carbon dioxide. Prior to the 1976-77 climate-shift, correlations between daily changes in atmospheric CO_2 and temperature anomalies for a single year are mostly positive (above normal temperatures cause the daily change in atmospheric CO_2 to be more positive), while after 1978 correlations are strongly negative (above normal temperatures cause CO_2 changes to be more negative). The reversal from positive to negative correlations after 1978 is caused by a steady increase in the number and size of positive temperature anomalies. Generally, correlations are positive before the climate shift and negative after the shift. The exceptions are the eruptions of El Chichon in 1982 and Mt Pinatubo in 1991, which weakened the CO_2-temperature link for 2-4 years following each eruption by reducing both the growth and decay rates of vegetation (Angell, 1997). The major El Nino events of 1982-83, 1997-98 and 2004-05 also affected vegetation growth and decay and altered the CO_2-temperature correlations for those years. Simulated versus observed seasonal cycles of CO_2 (the Keeling Curve) based on global temperature observations produce R^2 values that are over 0.90 for some years after 1978. The high negative correlation between CO2 change and temperature suggests that global temperature departures might now be predicted from the daily change in the concentration of atmospheric carbon dioxide.

Introduction

A unique shift in the global climate occurred during the winter season of 1976-77 (Miller, et al, 1994, Graham, 1994, Deser, 2006, Hartmann and Wendler, 2005, Smith and Reynolds, 2005). A composite data set of 40 environmental variables demonstrates an unequivocal step-like shift in the climate that occurred between the 1968-76 and 1977-84 periods (Ebbesmeyer et al, 1991). However, a consensus as to the underlying cause of the shift has not been reached (Karl, 1988, Karl and Trenberth, 2003). The International Panel on Climate Change emphasizes that " the detection of a change in climate does not necessarily imply that its causes are understood" (IPCC, 2007). The recent build-up of greenhouse gases is suspected as a cause but a clear cause and effect mechanism has not been found (Madden and Ramanathan, 1980, Hansen, et al, 1981, Ramanathan, 2006, Baines, 2007, Schlesinger et al, 2007). Unprecedented changes in atmosphere-ocean circulation and in sea-surface temperatures (SST) were observed in 1976 (IPCC, 2007). The high correlation between inter-annual variations in atmospheric carbon dioxide and the El Nino Southern Oscillation (ENSO) found for the 1965-2000 period suggests that increased CO_2 as one possible cause (Zeng, et al, 2005). Before the shift occurred, the equatorial Pacific Ocean had been identified as a region of CO_2 flux change that affects the development of ENSO (Bacastow, 1985). Annual anomalies of SST for 1850-2005 referenced to the 1961-90 period show an abrupt decline in negative anomalies after 1950 and a reversal from negative to predominantly positive in the late 1970s. (Rayner et al,2006, Smith and Reynolds, 2005). The 1976-77 regime shift also has had far reaching consequences for the large marine ecosystems of the North Pacific (Hare and Mantua, 2000). Warmer and drier conditions in Western North America significantly reduced the snowpack and runoff to record lows during the 1977 water year (Karl and Koscrlny, 1982). Precipitation in Western United States in 1976-77 still holds the record low in that region for the 20th century (Cayan and Peterson, 1989).

Input Temperatures

A gridded land-only data set of near-surface maximum and minimum temperature anomalies compiled by the Hadley Climate Center (HCC) provides the basis for this study. The HCC data set is derived from daily observations of maximum and minimum temperatures collected at approximately 6647 global weather stations selected by HCC using a rigorous quality-control procedure from an initial set of 15,000. (Caesar et al, 2006) Anomalies or departures from the normal temperature for each day are calculated using the reference period 1961-1990.

Table 1 INPUT TEMPERATURES (AVERAGED FOR 6647 GLOBAL STATIONS)

Symbol	Description
$TX_{(i,n,j)}$, $TN_{(i,n,j)}$	Daily maximum and minimum temperatures, for day i, year n and station j 1951-2008 period *
$TXB_{(i,j)}$, $TNB_{(i,j)}$	Mean daily maximum and minimum temperatures, for day i, and station j, averaged for the 1961-1990 period
$dTX_{(i,n,j)}$, $dTN_{(i,n,j)}$	Daily maximum and minimum temperature anomalies for day i, year n and station j, 1951-2008 period , equal to $dTX_{(i,n,j)} / TXB_{(i,j)}$ $dTN_{(i,n,j)} / TNB_{(i,j)}$

dTmax(i,n),dTmin(i,n) Daily maximum and minimum temperature anomalies averaged for 6647 global stations

* The water year (October 1-September 30) is used rather than the calendar year (January 1-Decmber 31) to avoid a divided winter season, therefore the full temperature record in this study begins in water year 1951, on October 1, 1950, and ends in water year 2008 on September 30. The same reasoning is used for the monthly carbon dioxide record, which now begins on October 1958 and ends on September 2008.

The HCC data set covers approximately 30% of the earth's total surface (land-only) area, therefore the results produced in this study may not be considered representative of the entire earth. However, an analysis of temperature changes using the 1850-1997 data set of monthly land and sea global temperatures (LST) collected by NOAA demonstrates that although the land stations show a greater variance of annual anomalies than the oceans, both have nearly identical time trends (Smith and Reynolds, 2005).

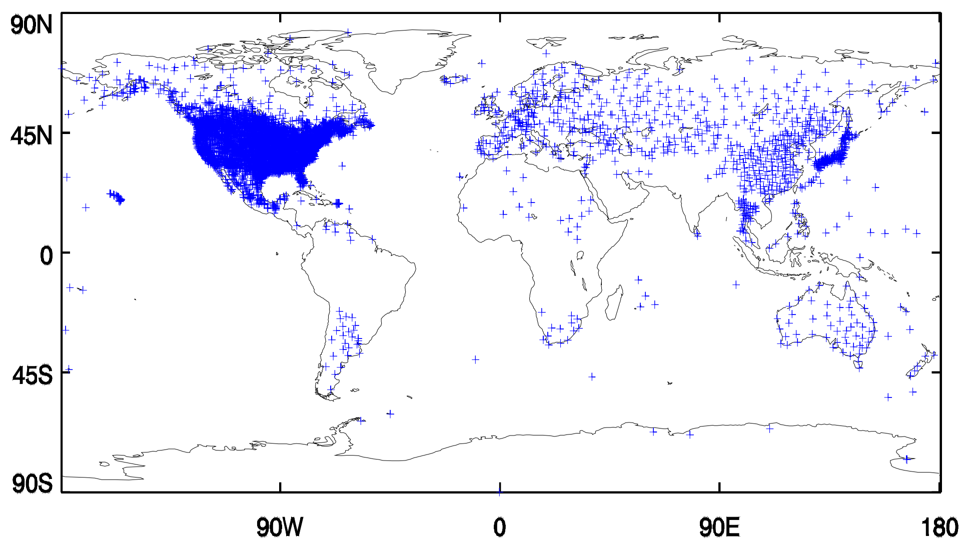

Figure 1a Location of 6647 Met stations used in the study (HadGHCND Data Set, Met Office Hadley Centre & US National Climatic Data Center). Period of record is 1950-2008; anomalies are referenced to the 1961-90 period.

Climate Shifts Demonstrated by Global Temperature Anomalies

A plot of cumulative temperature range anomalies, Σ (dTmax – dTmin), shown in Figure 1a suggests that the global climate shift in 1976-1977 may have altered how atmospheric carbon dioxide and surface air temperatures interact. It appears to have set the stage for a more significant climate shift in 2000 that enhanced the influence of temperature on the global biomass, thus affecting seasonal variations of atmospheric CO_2.

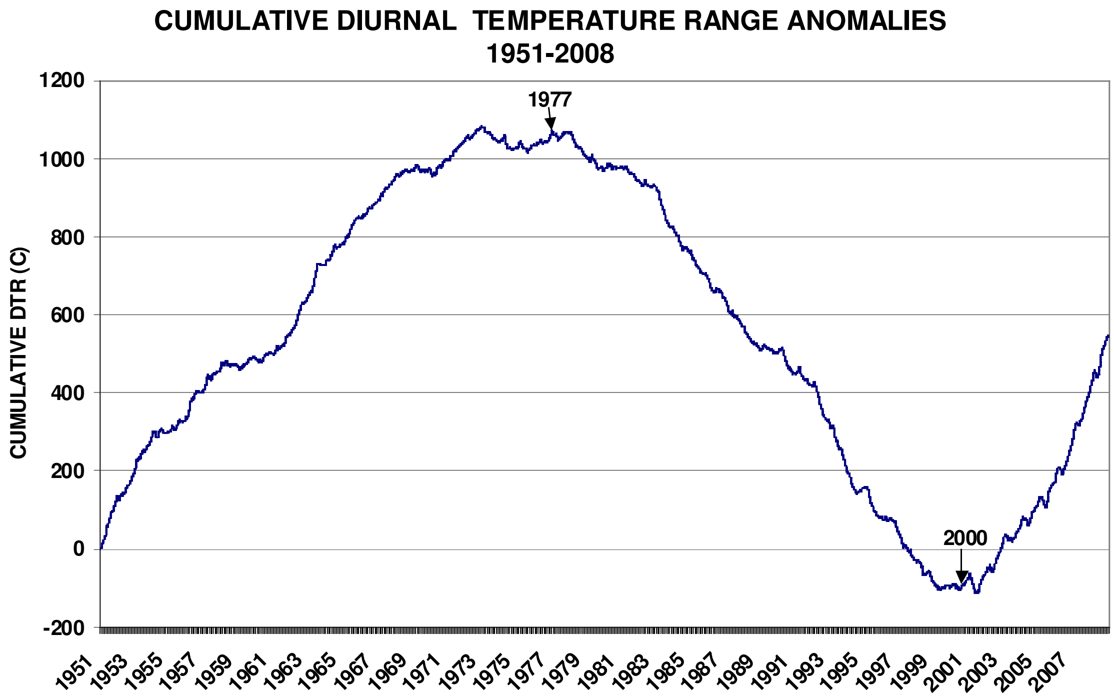

Figure 1b. Cumulative temperature range anomalies, Σ (dTmax – dTmin), for 1951-2008 reveals potential climate shifts in 1977 and 2000. The curve rises when positive maximum temperature anomalies are larger or occur more often than positive minimum anomalies and declines when positive minimum temperature anomalies occur more often than positive. The anomalies are based on daily departures from 1961-90 averages and are compiled by the Hadley Climate Center from temperature observations at 6647 weather stations worldwide.

The unusual winter season perturbations shown in Figure 1b (a subset of 1a) that appear only after the year 2000 indicate external climate forcing that is simultaneously affecting temperatures at most of the HCC global stations. There is strong similarity in the yearly timing (after the 1990s) and seasonal timing (December-January) to an earlier winter warming study (Tangborn, 2003), where it was found that beginning about 1990, positive temperature anomalies at nearly all of the global stations in the study were synchronized for a few days each January.

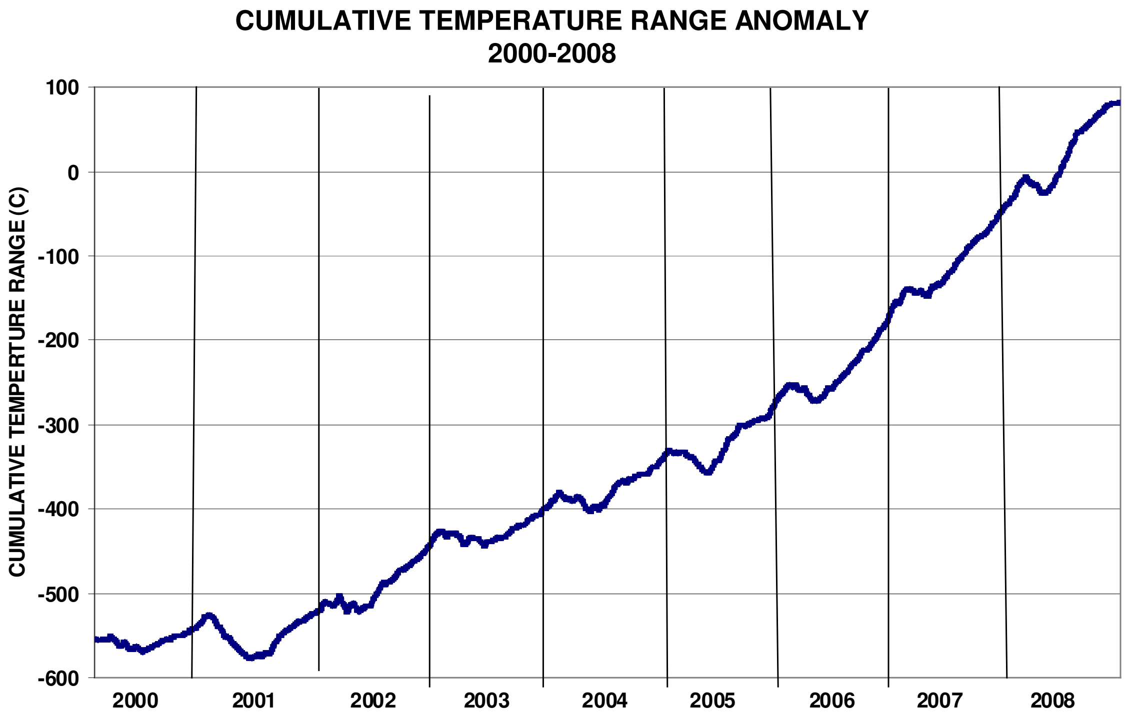

Figure 1c. Cumulative temperature range anomalies for 2000-2008, a subset of 1a. The subdued but regular cycles that appear each year are due to an abrupt increase in positive minimum temperature anomalies from approximately December 1 – January 31. The seasonal and yearly timing of these cycles is similar to the synchronized mean global temperature anomalies found in an earlier study of winter warming (Tangborn, 2003).

The cause of the abrupt switch after the year 2000 from the domination of positive maximum to the domination of positive minimum temperature anomalies on about December 1 may be due to a negative feedback mechanism that tends to retard a rapid rise in maximum temperatures. An increase in nighttime cloudiness due to a rise in atmospheric water vapor caused by increased evaporation would produce the increase in observed positive minimum temperature anomalies. The higher than normal maximum temperatures that occurred during the summer and autumn seasons after 2000 would produce an increase in ocean evaporation and cloudiness. If the minimum temperature increases shown in Figure 1b did not occur each December and January, the cumulative temperature range, dominated by maximum temperatures, would now be rising exponentially. Such an abrupt change (over a few days), occurring simultaneously each year at about the same time at over 6000 worldwide temperature stations is believed to be unprecedented.

The underlying cause for the change that has occurred in the pattern of global temperatures after 2000 is likely related to the comparatively recent rise in sea surface temperatures. From 1850 to 1980, except for a few years in the early 1940s, both land and sea surface anomalies (referenced to the 1961-90 period) were negative and had little variance. After the 1976-77 climate shift these anomalies are positive and more variable, and have been increasing steadily each year

(Brohan, 2006, Folland, 2003). The higher sea-surface temperatures have likely produced a diminution of the ocean-carbon sink, resulting in greater sensitivity of atmospheric carbon dioxide to temperature variations and their effect on the biosphere (Feeley et al, 2001, Sabine et al, 2005).
The distribution of temperature anomalies for the three delineated time periods shown in Table 2 reveal a distinct difference in the distribution of positive and negative anomalies between the 1951-77 and 2000-2008 periods.

TABLE 2 DISTRIBUTION OF TEMPERATURE ANOMALIES

PERIOD	NO.	RANGE		MAXIMUM		MINIMUM	
	DAYS	POS	NEG	POS	NEG	POS	NEG
1951 1977	9855	3796	6059	5303	4491	6006	3776
	FRACTION	0.39	0.61	0.54	0.46	0.62	0.38
1978 1999	8030	5214	2816	2983	5003	2196	5801
	FRACTION	0.65	0.35	0.37	0.63	0.27	0.73
2000 2008	3285	1058	2227	421	2860	468	2812
	FRACTION	0.32	0.68	0.13	0.87	0.14	0.86
1951 2008	21170	10068	11102	8707	12354	8670	12389
	FRACTION	0.48	0.52	0.41	0.59	0.41	0.59

Daily Change in Atmospheric Carbon Dioxide

Daily changes in carbon dioxide are reconstructed from monthly means derived from daily observations at Mauna Loa, Hawaii for 1958-2008 (Keeling, 1960, Keeling, et al, 1982). The conversion to a daily CO_2 format is necessary because daily interactions between temperature and carbon dioxide are obscured by monthly increments. However, for statistical analysis the number of independent values of CO_2 is considered to be 612 (one value per month).

The conversion to daily changes from changes in monthly means is by a 3-point interpolation technique. The predicted CO_2 concentration change for each day (from the previous day) of a specific month is found by weighting the observed change in monthly concentrations for the previous, current, and the subsequent month, based on the number of days to the 15^{th} of the current month, the date to which the published monthly means are adjusted.

For example, to find the daily CO_2 concentration change on July 10, the June monthly change from the previous month is inversely weighted by 25 days, the July change by 5 days and the August change by 36 days. The weight assigned to each month is found by:
$\mathbf{W = e^{-nf}}$, where n = number of days to the 15th and **f** is a coefficient, the value of which is found by minimizing the monthly reconstruction error.

The daily change in atmospheric carbon dioxide for day i and month m is equal to:

$$dCO_2\ (i,m) = W_1\ dCm_1 + W_2\ dCm_2 + W_3\ dCm_3$$

Where dCm1, dCm2, dCm3 are the monthly changes in concentration for the previous, current and subsequent month respectively. The values of f_1, f_2 and f_3 are 1.119, 0.646 and 0.160 when the minimum error for reconstructing the monthly concentration is attained. The estimated probable error for 612 monthly reconstructions is +/-0.23% or approximately +/- 0.77 ppm, the minimum error determined by this method.

The observed average daily change during the winter season (approximately November 1 to May 31), when CO_2 changes are positive for 11,272 days (62% of the time), is 0.0308 ppm per day with a standard deviation of 0.0124 ppm (+/- 40%); during the summer season (June 1 – October 31) the changes are negative for 6978 days (38% of the time) and the average is –0.0398 ppm per day with a SD of 0.02058 ppm (+/- 52%). The average (1959-2008) net influx of carbon to the atmosphere from the biosphere during the winter season is then 65.7 million tons per day (40.6 million tons per day averaged for the year). The average influx from the atmosphere to the biosphere during the summer is –84.8 million tons per day (-32.4 million tons per day averaged for the year). The average difference for the year (+ 40.6 – 32.4) is 8.2 million tons of carbon per day, produced by the burning of fossil fuel and deforestation. Thus approximately 20% of the daily influx of carbon to the atmosphere during the winter is produced by fossil fuels, the remainder is from vegetation decay in the biosphere.

The average daily change in atmospheric CO_2 can also be calculated by the average net daily influx of CO_2 to the atmosphere from October 1, 1958 to September 30, 2008 (18,250 days). The total concentration change for the full period is 69.85 ppm (382.7 – 312.85), and the total net influx is (69.85 /18,250) x 2130) = 8.15 million tons of carbon per day *.

* 1 ppm of atmospheric CO_2 = 2130 million tons of carbon

Figures 1a to 1h all pertain to the input data (atmospheric carbon dioxide and temperature anomalies) that are used in this study.

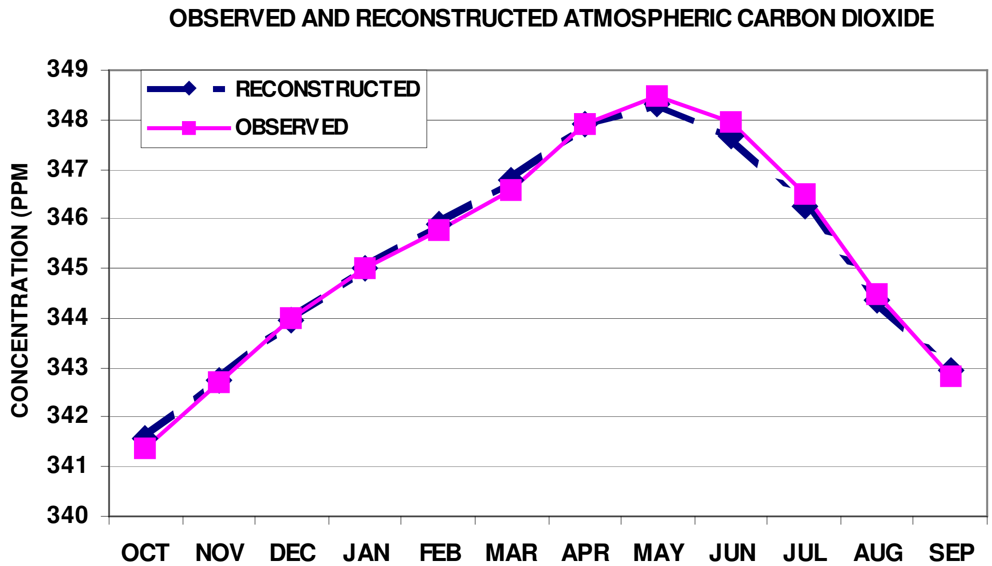

Figure 1d. Comparison of the reconstructed monthly concentrations of atmospheric CO_2 with the observed (averaged for 1959-2008) verifies the accuracy of the simulated dailies. The reconstructed monthly averages are calculated by summing the daily changes that were simulated from the initial measurements at Mauna Loa using a 3-point interpolation procedure and 3 coefficients. Based on this analysis the probable error for the daily change in CO_2 is approximately +/- 0.0002 PPM.

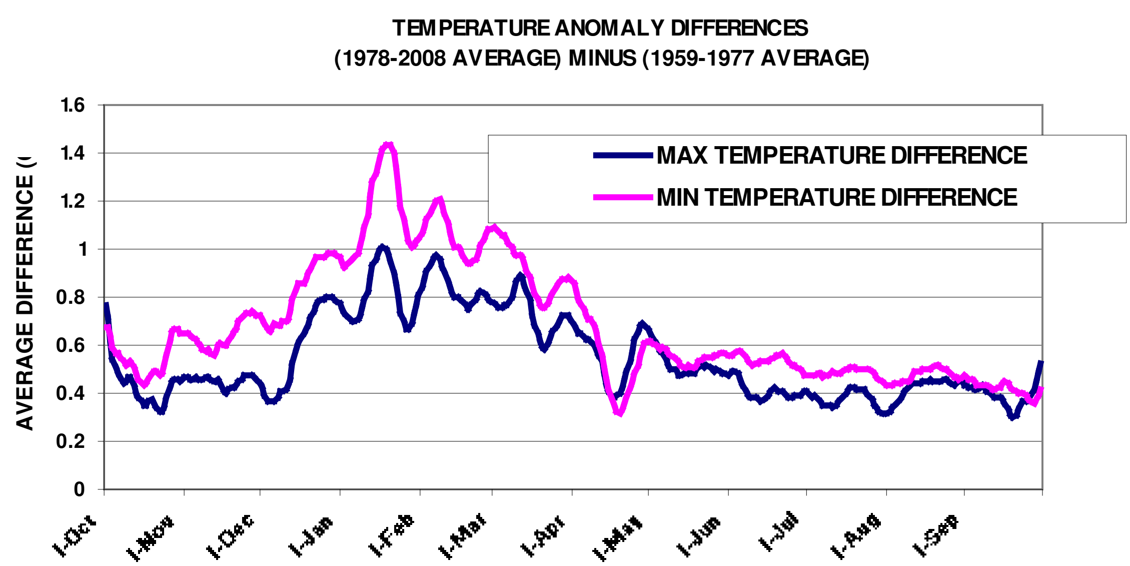

Figure 1e The difference in averaged temperature anomalies between the two periods separated by the 1976-77 climate shift. These differences demonstrate that both the maximum and minimum temperatures between the two periods increased throughout the

year. The minimum anomalies increased more than the maximums and both maximum and minimums increased more during the winter than the summer seasons.

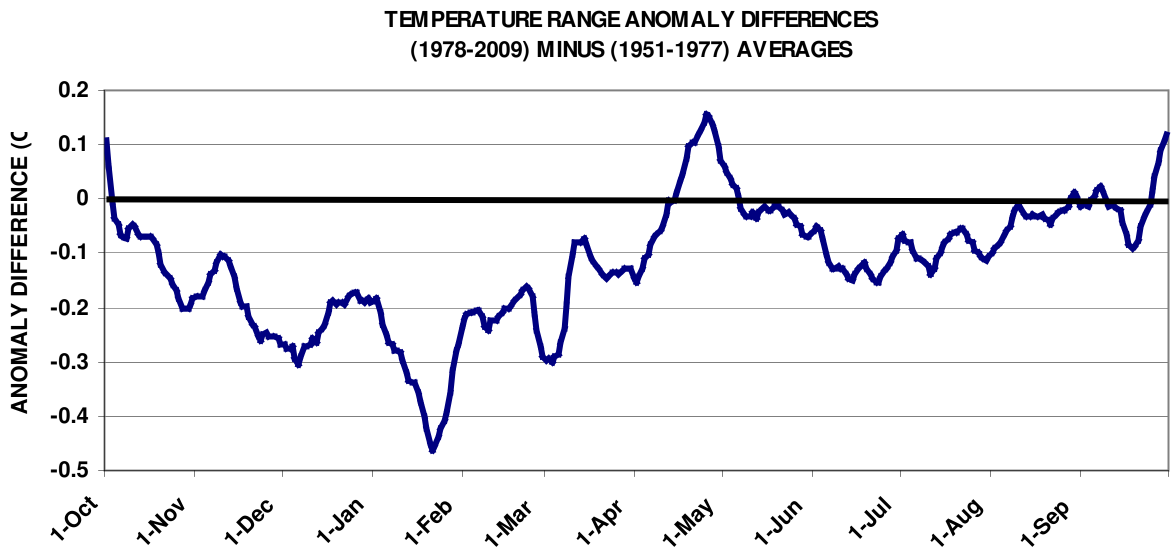

Figure 1f The difference in averaged temperature range anomalies between the two periods separated by the 1976-77 climate shift. These differences show that the temperature range anomaly (dTX – dTN) decreased throughout most the year between the two periods due to the number and size of minimum temperature anomalies usually being greater than the maximum.

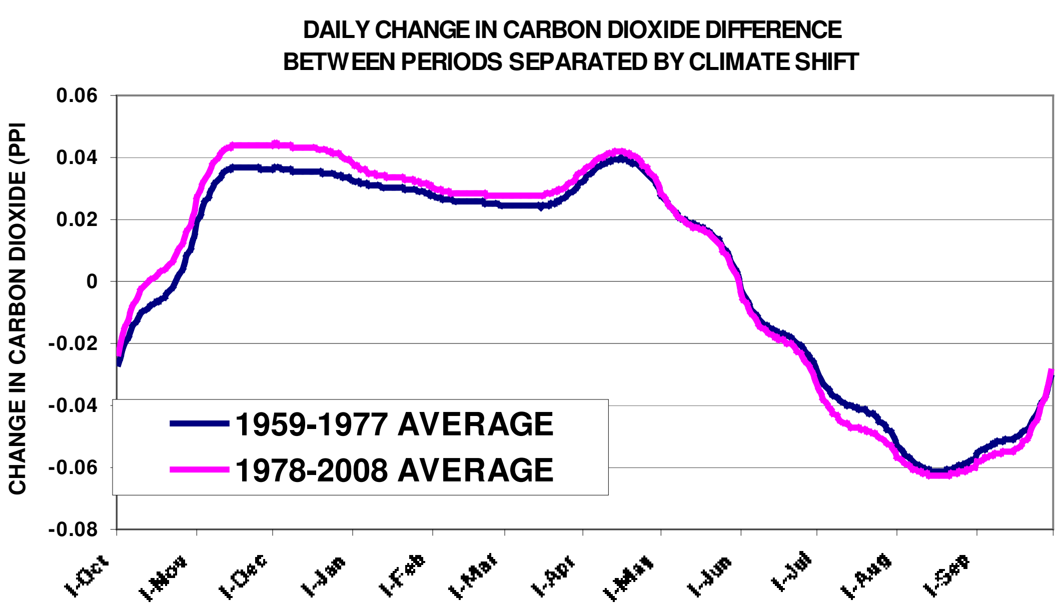

Figure 1g Daily change in CO_2 before and after 1976-77 climate shift. After 1978 changes were positive during the winter season and more negative in the summer. More positive winter changes indicate an increase in vegetation decay caused by higher temperatures and/or larger biomass. More negative summer changes indicate increase in vegetation growth caused by higher temperatures and/or larger biomass.

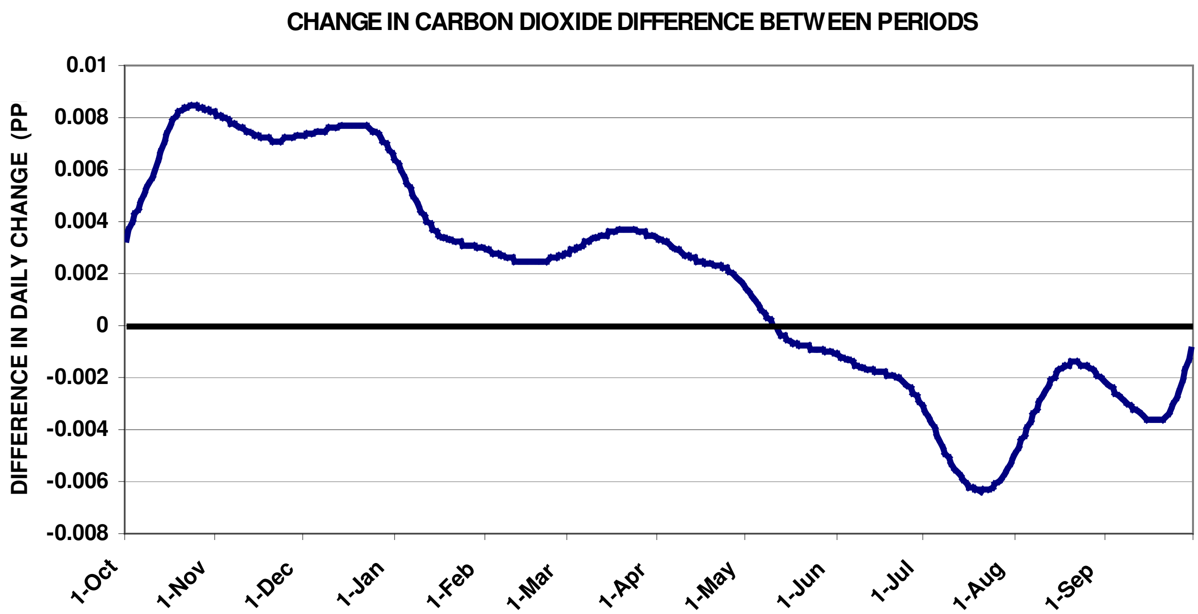

Figure 1h The change in the daily concentration of atmospheric CO_2 before and after the 1976-77 climate shift. Positive differences during the winter signify increased vegetation decay after 1978 from larger biomass and/or higher temperatures. Negative difference during the summer indicates that increased vegetation growth removing CO_2 from the atmosphere occurred at higher rate after 1978.

Linking Temperature and Atmospheric Carbon Dioxide

Following the 1976-77 climate shift, the diurnal temperature range (daily maximum minus daily minimum) has decreased significantly over much of the earth (Easterling *et al*., 1997). It is suggested that the declining DTR is an indication of increased vegetation growth (Myneni *et al.* 1997). Both increased concentrations of carbon dioxide and higher temperatures are likely responsible for the boost in global vegetation. The influence of vegetation on the response of the diurnal temperature to climate change has been demonstrated (Collatz, et al, 2000).

The diurnal temperature range equation (DTR = Tmax – Tmin) is modified to use daily maximum and minimum temperature anomalies for examining interactions between temperature and CO_2.

$$\mathbf{TR(i,n) = k_1\,(m)\,(dTmax\,(i,n)) - k_2\,(m)\,(dTmin\,(i,n))} \qquad \mathbf{(1)}$$

where TR(i,n) = modified temperature range anomaly on day (i), and year n dTmax(i,n), ddTn(i,n) = daily maximum and minimum temperature anomalies on day (i), k_1(m), k_2(m) = coefficients for month (m). The coefficients k_1 and k_2 adjust the maximum and minimum temperature anomalies to account for the difference between absolute temperatures and anomalies that are determined by the historic mean

Calibration to determine optimum values of k_1 and k_2 is by regression of daily changes in atmospheric CO_2 and the modified temperature range:

$$\mathbf{dCO(i,n) = \beta + \alpha\ TR(i,n)} \qquad \mathbf{(2)}$$

where dCO(i,n) is the observed daily change in atmospheric carbon dioxide, α and β are linear regression coefficients. Initially both k_1 and k_2 are assigned values of 1, then by minimizing the probable regression error by incrementally altering these coefficients by +/- 1% until the 1959-2008 average error is a minimum. The introduction of variable coefficients to the temperature range anomalies (equation 1) creates a slightly different approach for applying the diurnal temperature range to climate analysis. The temperature anomaly (departure from a long-term average) adds another dimension to routine daily temperature observations by incorporating a large amount of historical information into a single number.

Surface temperatures are in part controlled by the concentration of carbon dioxide in the atmosphere, and the daily change in carbon dioxide concentration is dependent on vegetation growth and decay, which is strongly influenced by surface temperatures. Thus there is a positive feedback loop between the daily change in carbon dioxide and temperature that is amplified as CO_2 levels increase.

The average annual prediction error determined for the 1959-2008 period is used as the objective function for determining optimum values of k_1 and k_2 that produce the minimum average error. For example, the objective function used for the 1959-2008 period is:

$$\mathbf{Eavg = \sum_{1959}^{2008} En\ N^{-1}} \qquad \mathbf{(3)}$$

where Eavg = average probable error for predicting daily change in CO2 based on the 1959-2008 period, En = error for year n, N = total number of years in the period.

CALIBRATION

Twenty-four coefficients (two per month), plus daily maximum and minimum temperature anomalies, form a temperature range index that is regressed against daily changes in atmospheric carbon dioxide. For each year 730 maximum and minimum anomalies are regressed against 365 daily changes in CO_2 using the 24 coefficients. The coefficients k_1 and k_2 are unchanged from year to year; the linear regression coefficients α and β vary slightly from one year to the next.

.

Final values of coefficients k_1 and k_2, shown in Figure 2a, indicate that during the summer growing season the maximum temperature is dominant for removing CO_2 from the atmosphere and the minimum temperature has little influence. During the winter season, when vegetation decay and fossil fuel burning are the sources of atmospheric CO_2, the daily minimum temperature exerts the largest influence and the effect of maximum temperatures is negligible.

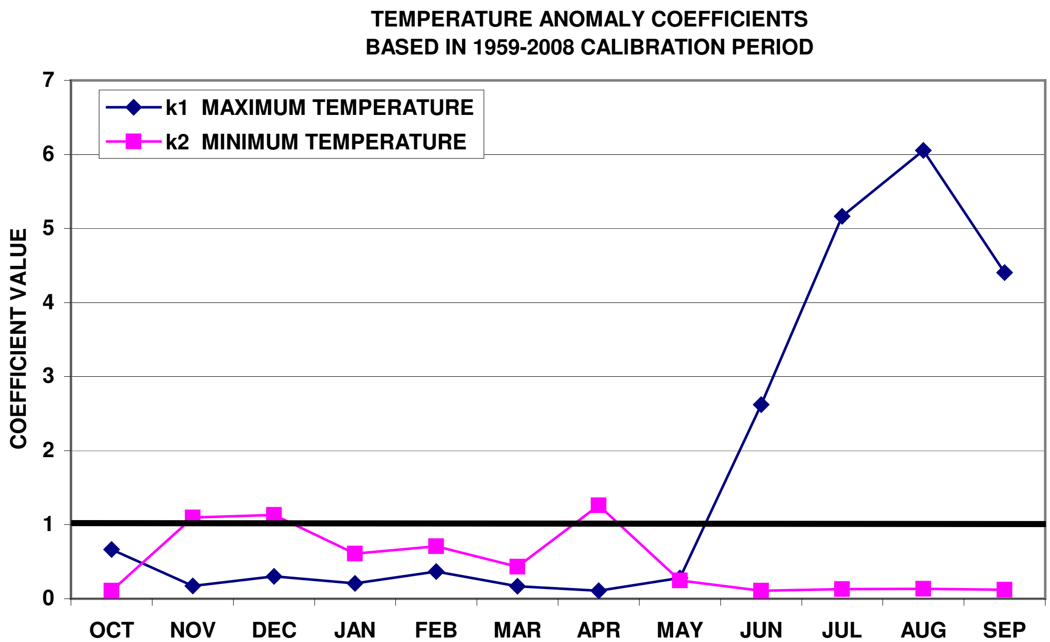

Figure 2a. Final values of coefficients k_1 and k_2 used in equation (1): $TR(i,n) = k_1 (m) (dTmax (i,n)) – k_2 (m) (dTn(i,n))$, to relate temperature to seasonal variations in carbon dioxide. TR(i,n) is the modified temperature range anomaly and dTmax and dTmin are daily departures from 1961-90 averages of daily maximum and minimum anomalies. Initially both k_1 and k_2 are assigned values of 1, then incrementally altered by +/- 1% (0.01) until the average error of dCO(i,n) versus TR(i,n) is a minimum (see Figure 2c).

The cause of the maximum temperature coefficient k_1 exceeding 1 for the summer months appears to be related to the time distribution of maximum and minimum anomalies. There is a significant change in the seasonal distribution of both k_1 and k_2 if the regression error of predicting CO_2 change from temperature is minimized for 2001-2008 rather than the 1960-2008 period (Figure 2b). For the shorter and more recent period, the maximum temperature coefficient becomes less dominant with the highest value reaching 3.5 in August, about half of its value for a 1959-2008 calibration. In addition, the minimum temperature coefficient, k_2, exceeds the maximum, k_1, for most of the winter and is nearly as high as the maximum, k2, in the month of June. Therefore, eliminating all of the years prior to the climate shift and two decades following the shift completely alters the character of the modified temperature range index (TR).

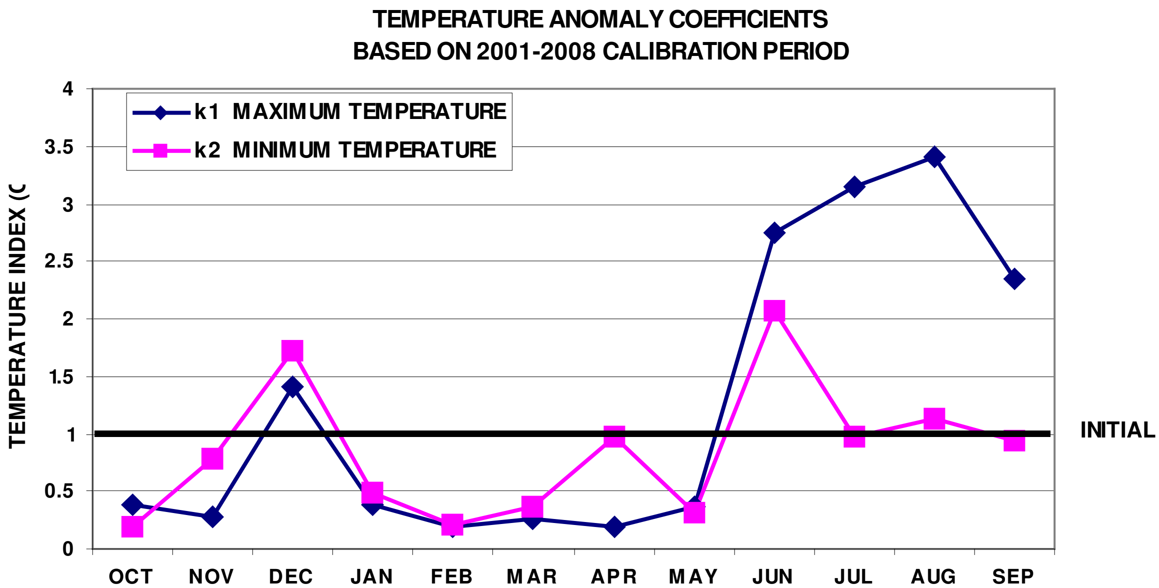

Figure 2b. Temperature anomaly coefficients based on 2001-2008 period calibration have a much different character than those calibrated for 1959-2008.

TR(i,n), is regressed against the observed daily change in the concentration of atmospheric carbon dioxide by:
$dCO(i,n) = \beta_n + \alpha_n TR(i,n)$, where dCO(i,n) = daily change in carbon dioxide, α_n and β_n are linear regression coefficients for year n (equation 2).
The average annual probable error for the 1959-2008 period is used as the objective function for optimizing k_1 and k_2 (equation 3).

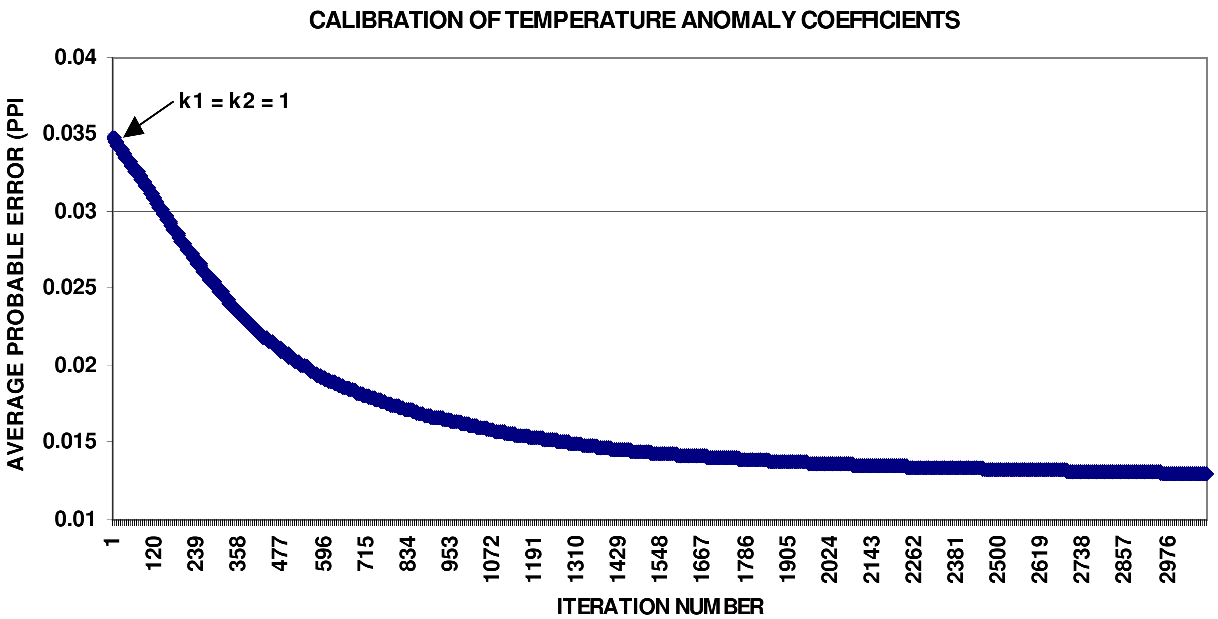

Figure 2c. Calibration of k_1 and k_2 coefficients in the equation $TR(i) = k_1 (m) (dTx (i)) – k_2 (m) (dTn(i))$ for the 2001-2008 period. When $k_1=k_2= 1$, TR(i) reverts to the temperature range equation. The values of k_1 and k_2 are alternatively changed by 0.01 for each iteration.

Figure 2c shows the average probable error during the calibration process to obtain optimal values of k_1 and k_2 to produce the minimum error for predicting daily CO2 change from temperature observations. The regression error is equal to 0.035 ppm (the correlation is near zero) when k_1 and k_2 are equal to 1 (at iteration # 1), then decreases as the linear fit between daily CO_2 change and temperature improves as k_1 and k_2 are incrementally altered by +/- 0.01 until the minimum regression error is reached.

The change in the concentration C of atmospheric CO_2 for day (i) is from the average concentration for 3 days prior to day (i), e.g. the concentration on June 15 is subtracted from the average concentration for June 12, 13 and 14.

$DCO2_i = C_i - (C_{i-1} + C_{i-2} + C_{i-3})/3$

Where:

C_i = concentration on June 15

C_{i-1} = concentration on June 14

C_{i-2} = concentration on June 13

C_{i-3} = concentration on June 12

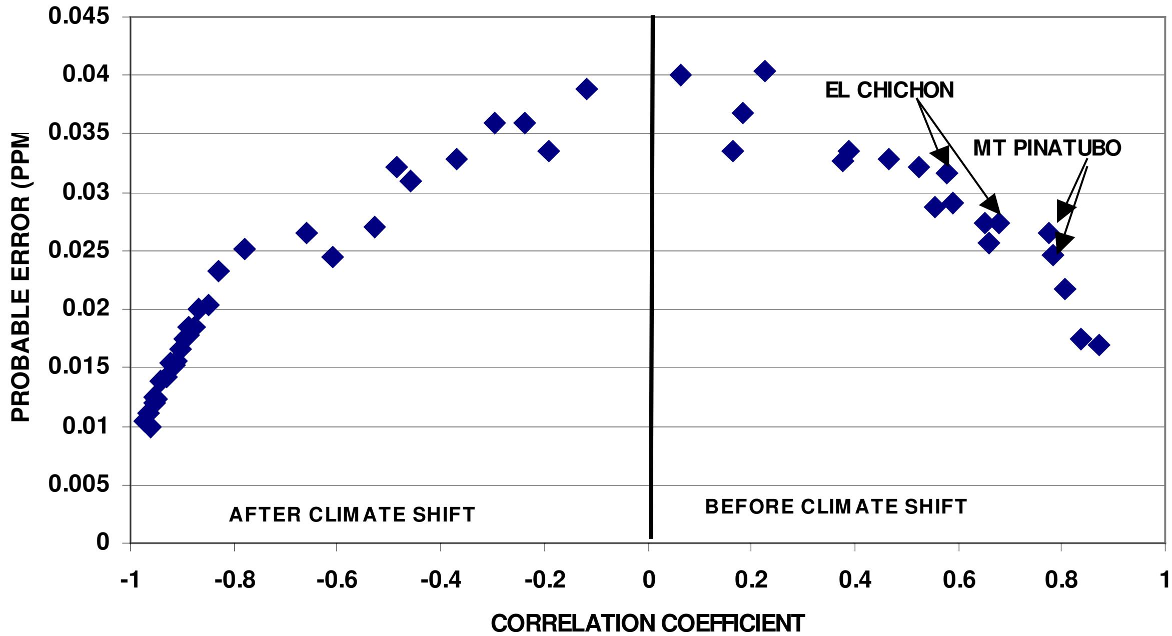

Figure 3. Probable error for predicting the daily change in CO2 from global temperatures versus the correlation coefficient. Generally the correlation is positive before the climate shift and increasingly more negative after the shift. The exceptions are for several years following the 1982 and 1991 eruptions of El Chichon and Mt. Pinatubo, and the 1997-98 El Nino.

The scatter diagram of probable error versus correlation shown in Figure 3 suggests that before the climate shift the correlation of CO_2 change and temperature was mostly positive and not strongly related to the regression error. After the shift and especially for approximately the past three decades, as the error of predicting CO_2 change from temperature decreases, the correlation and error are closely linked by a robust dependency, interrupted only by volcanic eruptions and strong ENSO episodes..

Time trends of daily dCO(i) and TR(i) after k_1 and k_2 are calculated are shown in Figure 4a for the 1959 – 1977 period prior to the climate shift.

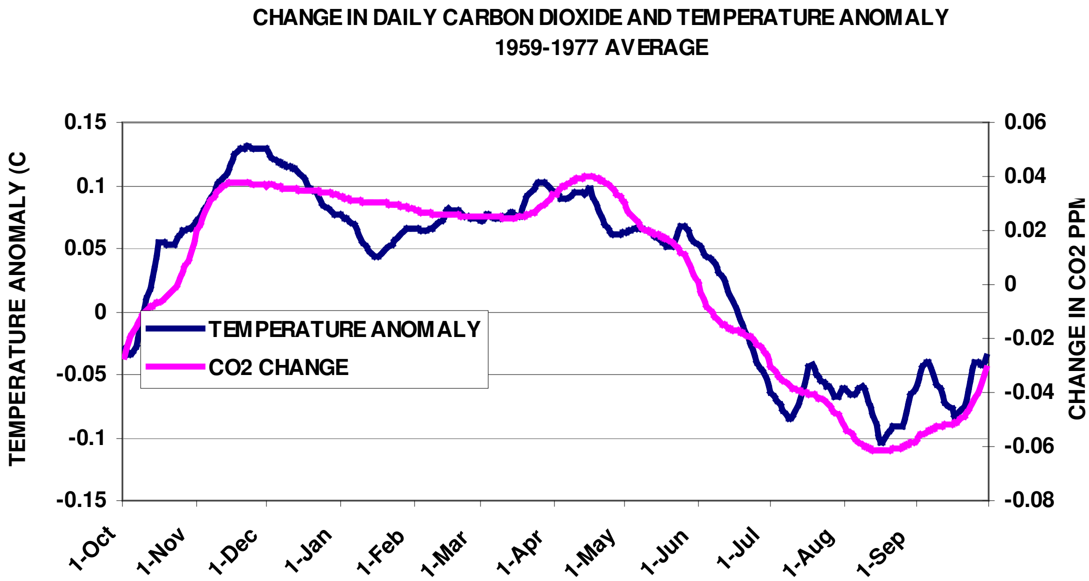

Figure 4a. Time-series of the daily modified temperature range anomaly (TR(i), generated from maximum and minimum temperature anomalies and the observed daily change in atmospheric carbon dioxide, dCO(i). Both temperature and CO2 change are positive during the winter season and negative during the summer.

The daily change in atmospheric CO_2 is positive from November-May in the Northern Hemisphere and is primarily due to the generation of carbon dioxide from vegetation decay, which increases with higher daily maximum temperatures but appears to be unaffected by minimum temperatures. The daily change in CO_2 is negative from June-October due to vegetation growth removing CO_2 from the atmosphere. Based on Figures 2a and 2b, above normal maximum temperatures appear to be more influential than daily minimums for enhancing vegetation growth during the summer.

Simulation of daily changes atmospheric carbon dioxide is accomplished by linear regression of observed daily changes in CO_2 (dCO(i)) to calculate α and β for each year. The modified temperature range anomaly TR(i), α and β are then applied to predict daily CO_2 changes, dSIM(i)

Conversion from the modified temperature range shown in Figure 4a to predicted CO2 change shown in 4b is by:

$$\mathbf{dSim(i) = \beta + \alpha\, TR(i)} \qquad \mathbf{(4)}$$

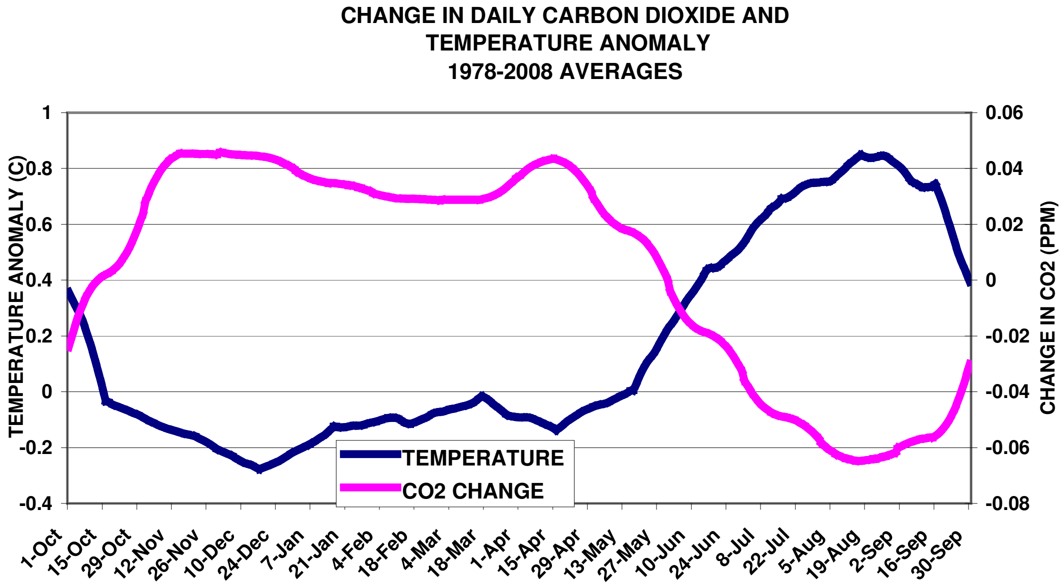

Figure 4b. Time series of observed change in atmospheric CO_2 from the previous day and modified temperature anomalies averaged for the 1978-2008 period. The pronounced change from 4a in the distribution and magnitude of daily temperature anomalies is inexplicable.

An improved understanding of the dependency of daily changes in atmospheric carbon dioxide to global temperatures may reveal how plant growth in the biosphere is controlled by temperature and carbon dioxide (Keeling et al, 1996). The dependency of CO_2 change on temperature before and after the climate shift, shown in Figures 4c and 4d, demonstrates the sensitive response of carbon dioxide concentration in the atmosphere to small changes in global temperatures.

Before the climate shift (1959-77, Figure 4c) and during the winter season (approximately November 1- May 31) when the change in daily CO_2 is nearly always negative, just slightly above normal temperatures produce positive changes (concentration of CO2 increases) due to increase in vegetation decay. An anomaly index of + 0.1 C causes the CO2 concentration to increase by 0.04 ppm. During the summer, a + 1 C minimum temperature anomaly (corresponding to a temperature anomaly index of –4 C) will boost vegetation growth and reduce atmospheric CO_2 by 0.02 ppm (5 million tons of carbon per day removed from the atmosphere and added to the biosphere).

After the climate shift conditions are reversed (Figure 4d). During the winter season below normal temperatures produce positive changes in atmospheric CO_2 due to suppression of vegetation decay. During the summer season, above normal temperatures stimulate vegetation growth causing CO_2 concentrations to decline.

The main difference between the two periods for the impact of temperature variations on the biosphere is the large increase in summer temperature indices caused by the high values of the maximum temperature coefficient k_1, resulting in a significant increase in the size of the biosphere.

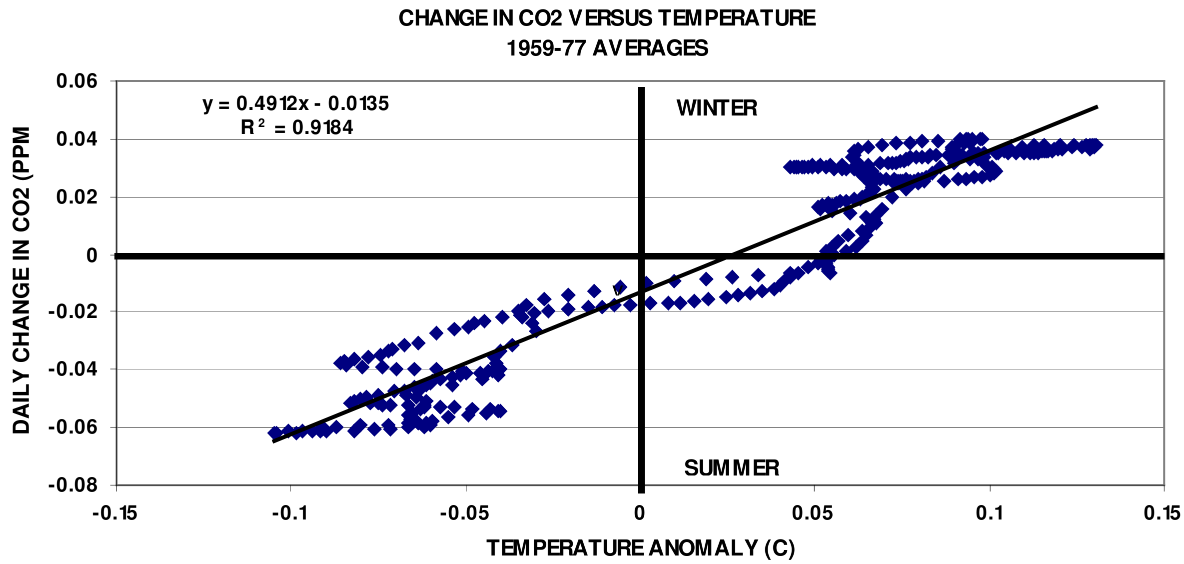

Figure 4c. Dependency of the observed change in atmospheric CO_2 (from the previous day) on the modified temperature anomaly index, averaged for the 1959-77 period and prior to the climate shift.

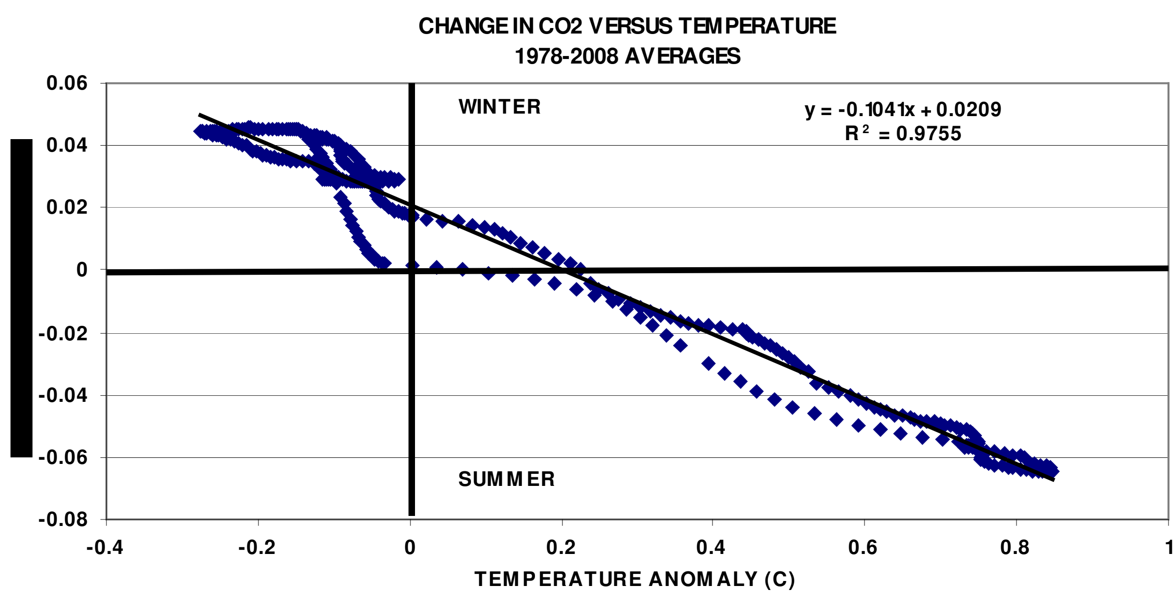

Figure 4d. Dependency of the observed daily change in atmospheric CO_2 (from the previous day) on the modified temperature anomaly index, averaged for the 1978-2008 period.

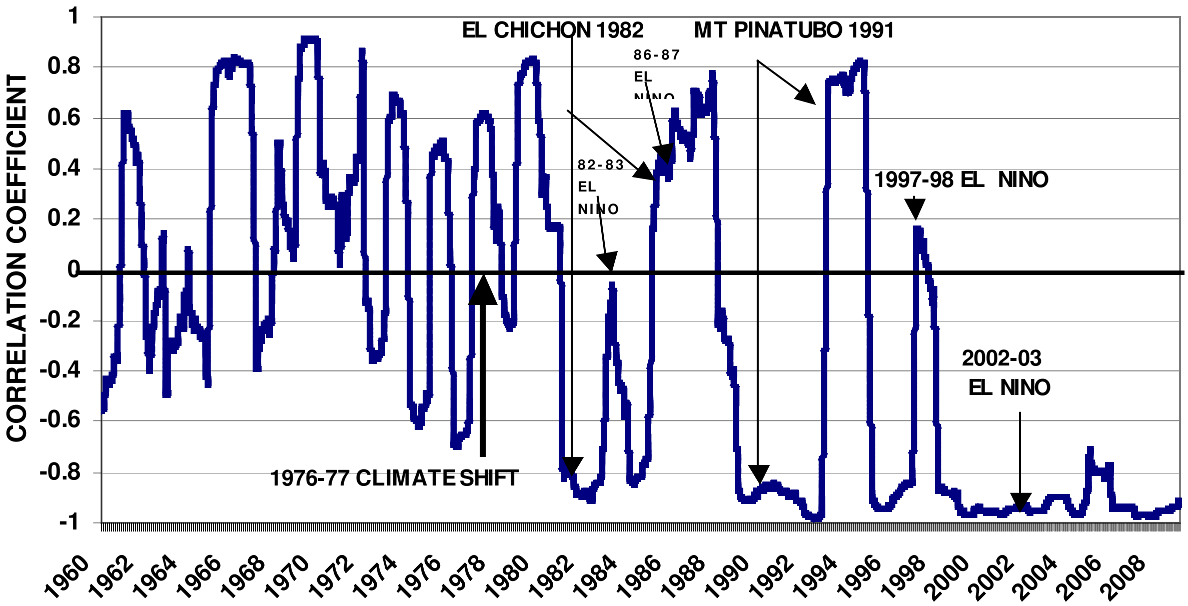

Figure 5. Correlation of the daily change in atmospheric carbon dioxide versus the modified temperature range for each year. Correlations are generally positive or slightly negative before the 1976-77 climate shift and increasingly negative after 1978, except for 3-6 years following two major volcanic eruptions, and the 1997-98 El Nino. Aerosols produced by the eruptions lowered global temperatures and impeded vegetation growth reducing the transfer of carbon dioxide from the atmosphere to the biosphere. Warmer oceans during the 1997-98 El Nino reduced the transfer of carbon dioxide from the atmosphere to the hydrosphere. Positive correlations indicate above normal temperatures coincide with positive changes in CO_2, mostly during the winter; negative correlations indicate above normal temperatures coincide with negative changes in CO_2, mostly during the summer and after 1978.

The volcanic eruptions of El Chichon in March 1982 and Mt Pinatubo in June 1991 reduced correlations due to cooling caused by volcanic aerosols (Hansen, et al, 1992). The lower temperatures following these eruptions affected vegetation growth and the reduced uptake of CO_2 by the biosphere (Post et al, 1996, Ramachandran et al, 2000). The correlation decline produced by the Mt Pinatubo eruption was similar to the El Chichon eruption but the cooling duration was shorter (Figure 5). However, the effect of the EL Chichon eruption is complicated by the 1986-87 El Nino. The average annual correlation of dCO2 and temperature changed from approximately +0.40 in 1959 to -0.90 in 2008.

Predicting Global Temperature Anomalies from Changes in CO_2

Simulation of atmospheric carbon dioxide changes directly from temperature observations emphasizes the sensitivity of the earth's climate to rising concentrations of all greenhouse gases. These results suggest that daily changes in atmospheric carbon dioxide can be predicted from temperature measurements with fair accuracy (that is steadily increasing). The next step is to reverse the process and apply the developed algorithms for predicting global temperature changes from increasing concentrations of carbon dioxide.

For the first (1959-1977) period, global temperature departures from the mean are dependent on daily changes in the concentration of atmospheric carbon dioxide by:

$DT_1 = 1.87\ (dCO2) + 0.028$

Or a + 0.01 ppm change in carbon dioxide (+21 billion tons of carbon per day) will raise the temperature 0.05 C.

For the second (1978-2008) period, temperatures are dependent CO2 changes by:

$DT_2 = -24.8\ (dCO2) + 0.656$

Or a +.01 ppm change raises the temperature 0.41 C.

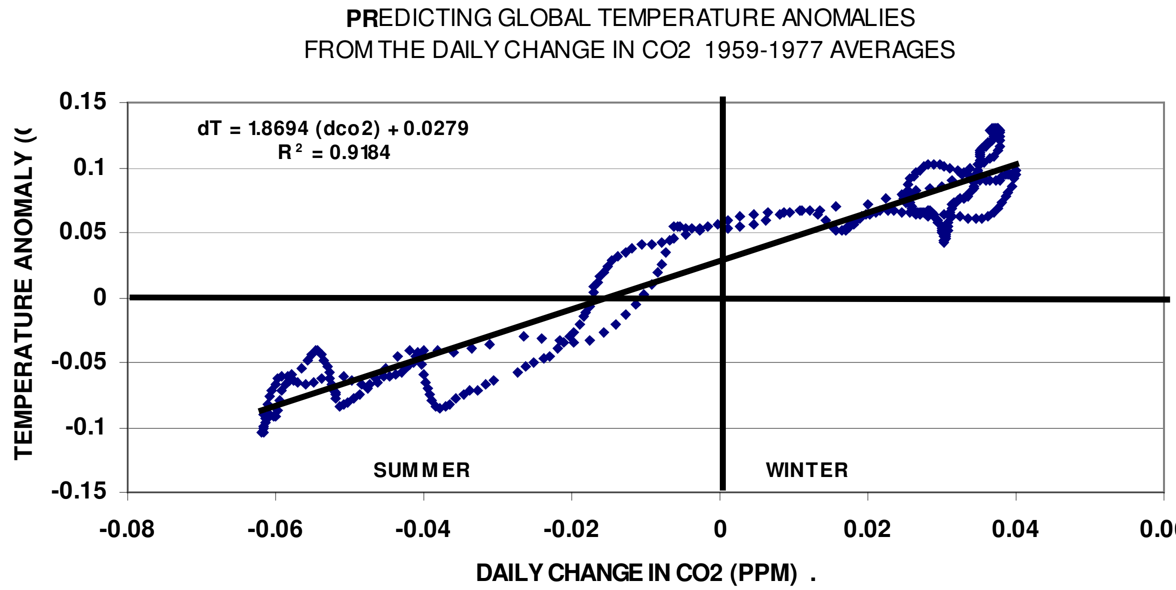

Figure 6a. Temperature change as a function of the change in carbon dioxide prior to the 76-77 climate shift.

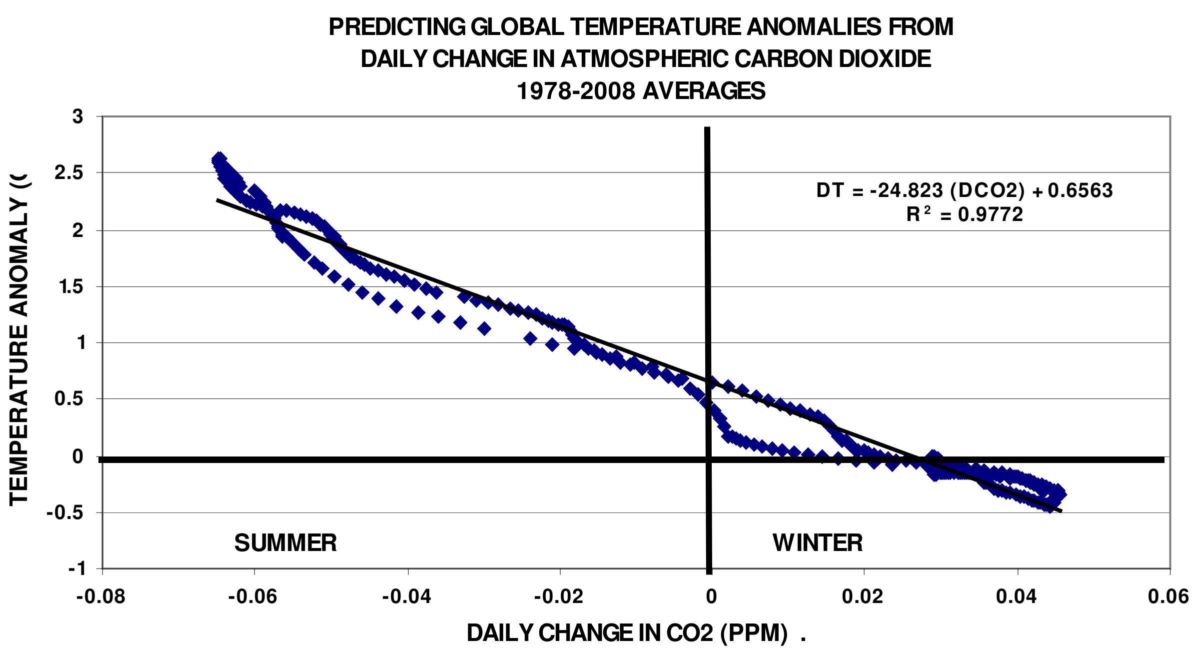

Figure 6b Temperature change as a function of carbon dioxide change following the 76-77 climate shift.

Simulation of the Keeling Curve

Estimating the daily concentration of CO2 from temperature anomalies is accomplished by the development of the relationship between temperature and the daily change in CO_2. Equation 4 (dSim(i) = β + α TR(i)) is applied for each year to simulate the daily change from the modified temperature index (TR(i)). Following the 1976-77 climate shift, the correlation between the daily CO2 change and temperature is increasingly more negative except after the two major volcanic eruptions and during the 1997-98 El Nino. The high R^2 (> 0.90) shown for linear regressions in predicting CO2 change from temperature for most years since 1992 is due to highly negative correlations caused by both increased vegetation growth during the summer and decay during the winter (Figure 7a). Simulating seasonal variations in CO_2 based on global temperatures will provide the means to verify the temperature – CO_2 change link (a low R2 indicates a disruption of the atmosphere-hydrosphere – biosphere balance from an external cause).

A comparison of observed and simulated concentration for 2007-08 is shown in Figure 7b. Both are constructed by summing the observed and simulated daily change from October 1 to September 30, with the observed concentration on October 1 as the initial point.

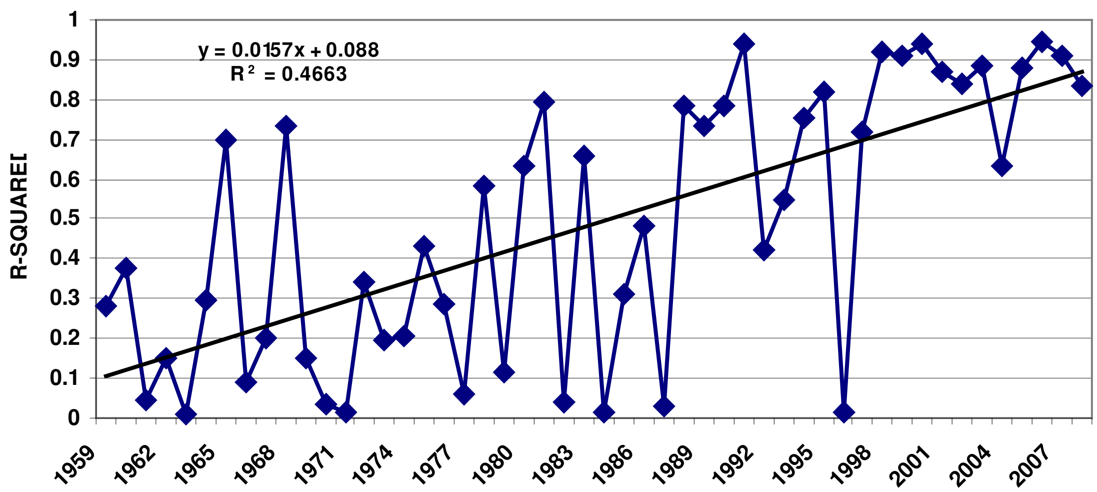

Figure 7a. R-squared for predicting the seasonal variations in the concentration of carbon dioxide from temperature observations. The effect of the two major volcanic eruptions in 1982 and 1991, and the 1997-98 El Nino is clearly shown, as is the 1976-77 climate shift.

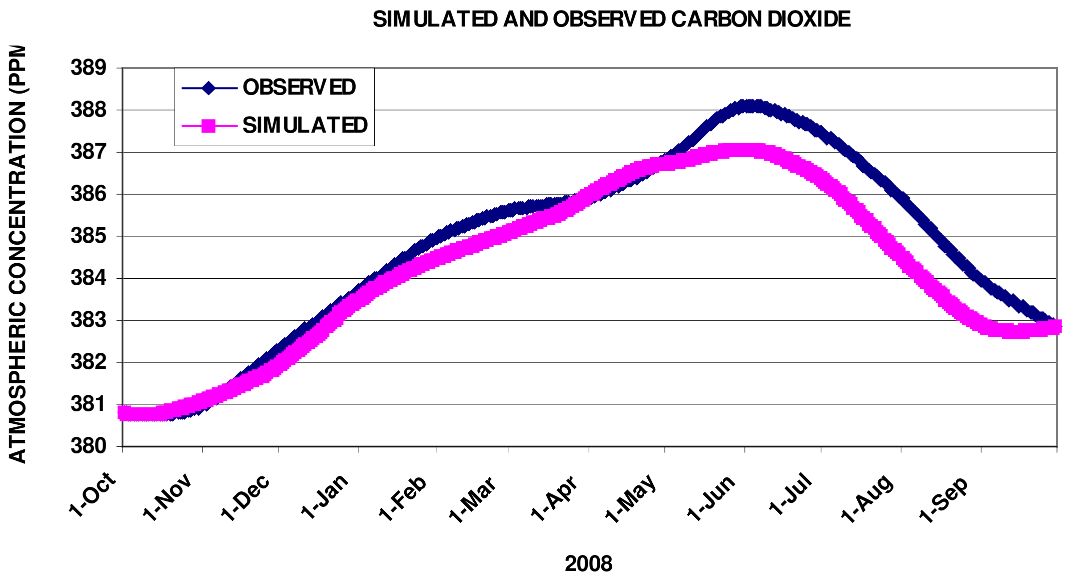

Figure 7b. Observed and simulated daily concentrations of atmospheric CO_2 for 2007-2008. The R^2 for a linear fit of observed and simulated concentrations is 0.96.

Main Results and Conclusions

The eight main findings resulting from this study are:

1. There is now a strong physical link between the daily change in atmospheric carbon dioxide and global temperatures that was weak or did not exist a half-century ago.
2. The daily change in the concentration of carbon dioxide can be quite accurately produced from the monthly concentration records.
3. A worldwide shift in the climate that occurred in the mid-to late 1970s has altered the balance of the atmosphere-hydrosphere-biosphere system, causing measureable changes in the interaction of carbon dioxide to the main components of the system.
4. The correlation between the daily change in CO2 and temperature anomalies reversed from weakly positive to strongly negative as an apparent consequence of the 1976-77 shift.
5. The eruptions of El Chichon in 1982 and Mt. Pinatubo in 1991 produced significant changes in the interaction between CO2 and temperature.
6. The major ENSO events can be detected by simultaneously monitoring global temperatures and atmospheric CO_2..
7. Estimating the seasonal Keeling Curve appears to be possible if major volcanic eruptions or ENSO events do not occur.
8. Predicting global temperature departures (and conceivably absolute temperatures) by monitoring the daily change in CO2 may be possible.

The reversal in the CO_2-temperature correlation after 1976-77 suggests a critical change occurred in the interaction of atmospheric carbon dioxide and temperature. The strong negative correlation for the past two decades, caused by a significant increase in summer temperature indices and/or increased vegetation growth, suggests global temperatures could now be predicted from daily changes in the concentration of carbon dioxide. Verification of these results with a General Circulation Model may reveal if the unpleasant surprises in the climate predicted over two decades ago will soon be a reality (Broecker, 1987).

Acknowledgements

Thanks to John Caesar of the Hadley Climate Center who compiled and provided the temperature data used in this study, to Andrew Tangborn for several critical reviews and unwavering support, and to Al Rasmussen for his usual incisive critiques. Funding for the project is provided by HyMet Inc.

References

Angell, J. K. (1997), Stratospheric warming due to Agung, El Chichón, and Pinatubo taking into account the quasi-biennial oscillation, J. Geophys. Res., 102(D8), 9479–9485

Baines, P.G. and C.K. Folland, 2007 Evidence for a Rapid Global Climate Shift across the Late 1960s, J. Climate, 20, 2721-2744

Bacastow, R.B., C.D. Keeling, and T.P. Whorf. 1985. Seasonal amplitude increase in atmospheric CO_2 concentration at Mauna Loa, Hawaii, 1959-1982. Journal of Geophysical Research 90(D6):10529-40.

Broecker, Wallace S. (1987). "Unpleasant Surprises in the Greenhouse?" Nature 328: 123-26

Brohan, P., et al, 2006, Uncertainty Estimates in Regional and Global Observed Temperature Changes: New Dataset from 1850, J. Geophys. Res., 111

Caesar, J., Alexander,L.,Vose,R. 2006 Large-scale changes in observed daily maximum and minimum temperatures: Creation of a new gridded data set. Journal of Geophysical Research, Vol 111, D05101

Collatz, G.J., Bounoua, L., Los, S.O., Randall, D.A., Fung, I.Y. and Sellers, P.J. 2000. A mechanism for the influence of vegetation on the response of the diurnal temperature range to changing climate. Geophysical Research Letters 27: 3381-3384

Deser, Clara (2006) Simulation of the 1976/77 Climate Transition over the North Pacific: Sensitivity to Tropical Forcing. Journal of Climate 19(23).

Easterling, D.R., Horton, B., Jones, P.D., Peterson, T.C., Karl, T.R., Parker, D.E., Salinger, M.J., Razuvayev, V., Plummer, N., Jamason, P. and Folland, C.K. 1997. Maximum and minimum temperature trends for the globe. Science 277: 364-367

Ebbesmeyer, C.C., D. R. Cayan, D. R. McLain, F. H. Nichols, D. H. Peterson and K. T. Redmond, 1991. 1976 step in the Pacific climate: forty environmental changes between 1968-1975 and 1977-1984. In J.L. Betancourt and V.L. Sharp [eds.], Proceedings of the Seventh Annual Pacific Climate (PACLIM) Workshop, April 1990. California Dept. of Water Resources. Interagency Ecological Studies Program Technical Report 26, 115-126

Feely, R., Sabine, C., Takahashi, T., Wanninkhof, R. (2001) Update and Storage of CO2 in the Ocean The Global CO2 Survey, Oceanography, Vol 14, No 4..

Folland,C.K, and Parker, D.E. 1990 Observed Variations of Sea surface Temperature. Climate-Ocean Interaction, M.E. Schlesinger, ed. Kluwer Academic Press, Dordrects, The Netherlands, 21-52.

Hansen , D. Johnson , A. Lacis , S. Lebedeff , P. Lee, D. Rind, and G. Russell. *Climate Impact of Increasing Atmospheric Carbon Dioxide* ***Science, 28 August, 1981, vol 213, no. 4511, pp 957-966.***

Hansen, J., A. Lacis, R. Ruedy, and M. Sato (1992), Potential climate impact of Mount Pinatubo eruption, Geophys. Res. Lett., 19(2), 215–218.
Hare, S.R.and NJ Mantua - Progress in Oceanography, 2000 - Elsevier

Hartmann, B. and Wendler, G., The Significance of the 1976 Pacific Climate Shift in the Climatology of Alaska", Journal of Climate, Vol.18, 2005)

Hegerl, G.C., F.W. Zwiers, P. Braconnot, N.P. Gillett, Y.Luo, J.A. Maerengo Orsini, N. Nicholls, J.E. Penner and P.A. Stott, 2007: Understanding and Attributing Climate Change, In Climate Change 2007: The Physical Basis. Contributions of Working Group I to the Fourth Assessment Report of the Intergovernmental Panel on Climate change.

Karl, T., and A. Koscielny, Drought in the United States: 1895-1981, J. Climatol., 2, 313-329, 1982

Karl, T., and K. Trenberth (2003) Modern Global Climate Change, Science, Vol 302, 5 December 2003

Keeling C.D., The Concentration and Isotopic Abundances of Carbon Dioxide in the Atmosphere, Tellus, 12, 200-203, 1960

Keeling, C.D., R.B. Bacastow, A.E. Bainbridge, C.A. Ekdahl, Jr., P.R. Guenther, L.S. Waterman, and J.F.S. Chin. 1976. Atmospheric carbon dioxide variations at Mauna Loa Observatory, Hawaii. Tellus 28(6):538-51.

Keeling, C.D., R.B. Bacastow, and T.P. Whorf. 1982. Measurements of the concentration of carbon dioxide at Mauna Loa Observatory, Hawaii. In W.C. Clark (ed.), Carbon Dioxide Review: 1982. Oxford University Press, New York.

Keeling, C.D., J.F.S. Chin, and T.P. Whorf. 1996. Increased activity of northern vegetation inferred from atmospheric CO_2 measurements. Nature 382: (6587) 146-49. MacMillan Magazines Ltd., London.

Khatiwala ,S., Primeau,F., Hall,T. 2009. Reconstruction of the history of anthropogenic CO2 concentration in the ocean. Nature 462. MacMillan Magazines Ltd., London.

Madden, R.A. and V. Ramanathan, 1980, Detecting Climate Change due to Increasing Carbon Dioxide, **Science** ***Vol. 209. no. 4458, pp. 763 - 768***

Miller, A.J., D.R. Cayan, T.P. Barnett, N.E. Graham and J.M. Oberhuber, 1994. The 1976-77 climate shift of the Pacific Ocean. Oceanography 7:21-26.

Park, Jeffrey (2009),A re-evaluation of the coherence between global-averaged atmospheric CO_2 and temperature at inter-annual time-scales, GRL VOl 36.

Post, M. J., C. J. Grund, A. M. Weickmann, K. R. Healy, and R. J. Willis (1996), Comparison of Mount Pinatubo and El Chichon volcanic events: Lidar observations at 10.6 and 0.69 µm, J. Geophys. Res., 101(D2), 3929–3940.

Myneni, R.C., Keeling, C.D., Tucker, C.J., Asrar, G. and Nemani, R.R. 1997. Increased plant growth in the northern high latitudes from 1981 to 1991. Nature 386: 698-702.

Ramachandran, S., V. Ramaswamy, G. L. Stenchikov, and A. Robock (2000), Radiative impact of the Mount Pinatubo volcanic eruption: Lower stratospheric response, J. Geophys. Res., 105(D19), 24,409–24,429.

Sabine, C.L., Feely, R., Gruber, N., Key, R., Lee, K., Bullister, J., Wanninkhof, R., Wong, C.,S., Wallace, D., Tilbrook B., Millero, F., Peng, T., Kozyr, A., Ono, T., and. Rios, A .The Oceanic Sink for Anthropogenic CO_2 **Science** ***16 July 2004 305: 367-371***

Schlesinger M.E., Haroon S. Kheshgi, Joel Smith, Francisco C. de la Chesnaye, John M. Reilly, Tom Wilson, Charles Kolstad, Human-Induced Climate-Change, Cambridge University Press

Swanson, K. L., and A. A. Tsonis (2009), Has the climate recently shifted?, Geophys. Res. Lett., doi:10.1029/2008GL037022, in press.(accepted 24 February 2009)

Smith, T.M., and R.W.Reynolds, 2005: A global merged land air and sea surface temperature reconstruction based on historical observations (1880-1997)). J. Clim.

Smith, T.M., R.W. Reynolds, T.C. Peterson, and J. Lawrimore 2007: Improvements to NOAA's Historical Merged Land-Ocean Surface Temperature Analysis (1880-2006). J. Clim.

Tangborn, W.V. 2003 Winter warming indicated by recent temperature and precipitation anomalies, Polar Geography, 27, No. 4, pp320-338

Solomon,S.,et.al, Climate Change, 2007 - The Physical Science Basis, (Cambridge University Press, 2007)

Trenberth, K. E.,, 1990: Recent observed interdecadal climate changes in the Northern Pacific. Bull. Am. Meterol. Soc.71, 988-993.,

Trenberth, K. E., and D. P. Stepaniak, 2001: Indices of El Niño evolution. J. Climate., 14, 1697-1701. [Paper(.pdf)] *

Trenberth, K. E., and D. J. Shea, 2005: Relationships between precipitation and surface temperature. Geophys. Res. Lttrs., 32, L14703, doi:10.1029/2005GL022760.[Paper (.pdf)]

Trenberth, K. E., and A. Dai, 2007: Effects of Mount Pinatubo volcanic eruption on the hydrological cycle as an analog of geoengineering. Geophys. Res. Lttrs., 34, L15702, doi:10.1029/2007GL030524. [PDF

Zeng, N., A. Mriotta, and P. Wetzel (2005), Terrestial mechanisms of interannual CO2 variability, Global Biogeochem. Cycles,19, GB1016